Continuous Protein Recovery with a Liquid–Solid Circulating Fluidized-Bed Ion Exchanger

Qingdao Lan, Amarjeet S. Bassi, Jing-Xu (Jesse) Zhu, and Argyrios Margaritis
Dept. of Chemical and Biochemical Engineering, University of Western Ontario, London, Ontario, Canada N6A 5B9

A liquid–solid circulating fluidized-bed (LSCFB) ion-exchange system was developed for continuous protein recovery. It contains a downcomer for protein adsorption and a riser for protein desorption, with ion-exchange particles circulating continuously between the two columns. Effects of the operating conditions on the hydrodynamics and the continuous ion exchange of bovine serum albumin (BSA) in the system were investigated. Under typical operating conditions, up to 98% BSA was adsorbed in the downcomer (showing a very high efficiency of protein removal from the feed), and an overall protein recovery of up to 84% was obtained in the LSCFB system, indicating that the LSCFB system was a very promising strategy for the continuous recovery of proteins.

Introduction

The simplification of downstream treatment is one of the key factors contributing to the cost reduction of a biological production process. This may be achieved by the integration of separate single steps into a new unit operation or by using continuous rather than batch operations. A typical biological broth usually contains a large amount of very small solids and relatively low concentrations of the desired product. The first task in developing suitable downstream processing operations is to focus on the selection of an appropriate procedure for handling the solids present in the broth, for example, filtration or centrifugation. However, the presence of colloidal solids, such as cell debris, and the viscous properties of biological broth frequently make both of these methods costly and inefficient.

Whole broth extraction using a fluidized-bed ion-exchange system is a good strategy for downstream treatment, as it eliminates the difficult solids separation step and recovers the desired products directly from unclarified whole broth. The large bed voidage of a fluidized bed allows the particulates in the feed to pass through the bed while retaining the ion-exchange particles in the bed (Draeger and Chase, 1991; Chase, 1994). Continuous ion exchange using different fluidized-bed systems has been extensively investigated (Turner and Church, 1963; Higgins, 1969; Slater and Prud'homme, 1972; Porter, 1975; Himsley, 1981; Pungor et al., 1987; Gordon et al., 1990; Rodrigues et al., 1992; Byers et al., 1997). Burns and Graves (1989) applied a two-column magnetically stabilized fluidized-bed system for the continuous chromatography of biochemical products. Those authors, however, treated the system as comprising two identical columns, and no discussion was provided regarding the transportation of ion-exchange particles between those two columns. In addition, the operation of the magnetically stabilized fluidized-bed system was complicated and costly. Gordon et al. (1990) reported on the continuous affinity recycle extraction (CARE) of proteins using two well-stirred reactors. This system, although simple and easy to control, has the disadvantage of low ion-exchange efficiency and the requirements of large processing volumes even for a moderate throughput. Himsley (1993) patented a continuous countercurrent ion-exchange process from a feed liquor containing ions that, when absorbed, caused the density of the particles to increase. However, this device was designed only for the adsorption. The other operations of an ion-exchange process, that is, desorption, washing, and regeneration, were still carried out in a conventional packed-bed process.

Zhu et al. (2000) proposed a liquid–solid continuous fluidized-bed (LSCFB) system as a potentially excellent candidate for the continuous recovery of proteins from unclarified whole broth. The proposed LSCFB system is a continuous operation with simultaneous adsorption and desorption (regeneration) being carried out in the two separated fluidized beds, the downcomer and the riser. The ion-exchange parti-

Correspondence concerning this article should be addressed to A. Bassi.

Table 1. Properties of Diaion HPA25 Ion-Exchange Particles

Matrix	Polystyrene (highly porous)
Functional group	Quaternary alkylamine
Ionic form	Cl^{-1}
Average diameter (d_p, mm)	0.32
Wet density ρ_s, g/mL)*	1.08
Total exchange capacity Cl^-, meq/mL)	0.6
Terminal velocity (U_t, mm/s)	4.5
Bed expansion index (n)	2.67
BSA adsorption capacity (q_m, kg/m^3)	87.9

cles circulate continuously between the two columns. The introduction of a liquid–solid circulating fluidized bed opens the possibility of developing an integrated unit operation that recovers products from the unclarified whole broth directly and continuously. The LSCFB offers the advantages of a conventional fluidized bed, for example, the applicability to unclarified whole broth and the low pressure drops.

In a previous article, the authors introduced the concept of the LSCFB system and modeled the adsorption and desorption process (Lan et. al., 2000). The isothermal characteristics and the kinetics of BSA adsorption onto Diaion HPA25 in a finite bath have been reported in previous articles (Lan et al., 2001; Rowe et al., 1999). The objective of the current work is to study the hydrodynamics of the system and to investigate the parameters affecting the protein recovery using a model protein, bovine serum albumin (BSA).

Materials and Methods

Materials

Bovine serum albumin (BSA) (Sigma Chemical Co., St Louis, MO) was used as model protein. Anion-exchange particles Diaion HPA25 (Sigma Chemical) were used for all hydrodynamic studies and for the BSA adsorption/desorption studies. The properties of Diaion HPA25 particles are listed in Table 1. Phosphate buffer of pH 7.0 (10 mM) was used for all adsorption/desorption studies. Hydrodynamic studies were conducted using tap water as the fluidization liquid.

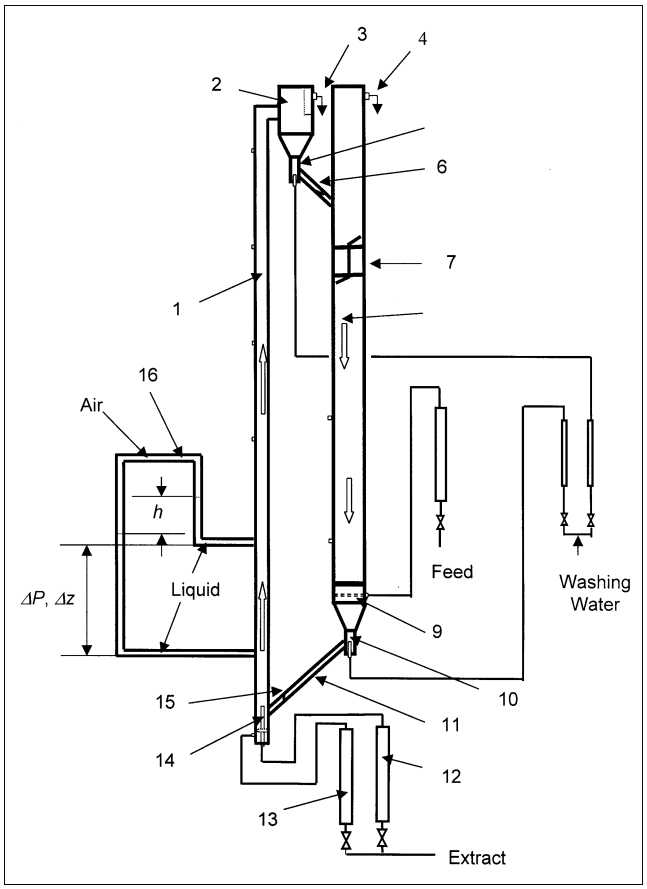

Figure 1. Liquid–solid circulating fluidized-bed (LSCFB) ion-exchange system.

1. Riser; 2. liquid-solids separator; 3. extract outlet; 4. raffinate outlet; 5. top washing section; 6. top solids return pipe; 7. solids circulating-rate measuring device, 8. downcomer; 9. distributor of the downcomer; 10. bottom washing section; 11. bottom solids return pipe; 12. the primary stream in the riser distributor; 13. the auxiliary stream in the riser distributor; 14. liquid distributor of the riser; 15. butterfly valve; 16. pressure manometer.

Experimental apparatus

As shown in Figure 1, the major components of the LSCFB system included the riser (1), a downcomer (8), a liquid–solid separator (2), a top solids return pipe (6), a bottom solids return pipe (11), a top wash section (5), and a bottom wash section (10). The riser was 3.0 m tall and 38.0 mm in diameter, and the downcomer was 2.5 m tall and 120.0 mm in diameter. Two separate liquid streams were used to fluidize the particles in the riser and the downcomer while the particles circulated between the two columns. The riser was operated in the entrained flow regime and the downcomer in the conventional fluidization regime. To secure the pressure balance between the riser and the downcomer, which is very important for the stable operation of an LSCFB system (Zheng and Zhu, 2000), the liquid outlets on the top of the downcomer and the separator were located at the same level. The distributor for the downcomer was a tubular ring that was carefully designed in order to have a uniform liquid distribution while allowing the solids to flow through.

The distributor for the riser (14) was designed so as to divide the incoming stream into two substreams: the primary and the auxiliary streams. The primary stream entered through a tubing of 1.1 cm in ID extending 5.1 cm into the riser. The outlet of the primary stream was located above the solids entrance at the bottom of the riser. This design helped to increase the pressure drop across the bottom solids return pipe and made the system more stable. The purpose of the auxiliary stream was to mobilize the particles at the bottom, which were then entrained up the riser by the combination of the primary and the auxiliary streams.

The solids circulation rate in this apparatus was controlled by a butterfly valve located on the bottom solids return pipe. This mechanical valve was preferred over the hydraulic valve described by Zheng et al. (1999) due to the low density of the Diaion HPA25 anion-exchange particles, which made the operation of a hydraulic valve difficult.

The solids circulation rate was measured by a device that consisted of a central vertical plate and two half butterfly

valves (7). The central plate divided the column into two halves and the two butterfly valves were fixed at the top and the bottom of the two half-sections. By appropriately flipping over the two valves from one side to the other, particles circulated through the system could be accumulated in one side of the measuring section for a specific period of time to calculate the particle circulation rate. The pressure gradient in the riser and the downcomer was measured using pressure manometers (16).

The dynamic seals between the riser and the downcomer were achieved by maintaining the two solids return pipes in the moving packed-bed regime. The top wash section and the bottom wash section rinsed the particles before entering the solids return pipes and helped to dilute and prevent the intermixing of the liquids from the riser and the downcomer sections.

Continuous BSA Ion Exchange in the LSCFB System

Continuous BSA ion-exchange in the LSCFB system was carried out with a 2-g/L BSA solution as feed and a 0.4-M NaCl solution as the extracting buffer unless otherwise indicated in the text. Both the BSA and NaCl solutions were prepared in 10 mM, pH 7.0 phosphate buffer. Other conditions are indicated in the text. In the continuous BSA ion-exchange studies in the LSCFB, the feed protein solution was introduced from the tubular distributor into the bottom of the downcomer. The regenerated Diaion HPA25 ion-exchange particles were introduced from the top solids return pipe into the top of the downcomer. The liquid velocity was controlled in such a way that the downcomer operated in the conventional fluidized regime (liquid velocity in the downcomer was maintained lower than the terminal velocity of the ion-exchange particles), where the ion-exchange resin particles moved down countercurrent to the rising feed liquid. As the particles and feed contacted countercurrently in the downcomer, the BSA in the feed was adsorbed onto the ion-exchange particles. The deproteinized solution was discarded from the top of the downcomer. The loaded particles were then transferred to the bottom of the riser through the bottom solids return pipe after washing. The extracting buffer (0.4 M NaCl solution in 10 mM pH 7.0 phosphate buffer) was applied from the bottom of the riser. The superficial velocity in the riser (U_{lr}), which was the combination of the primary and the auxiliary streams, was kept higher than the terminal velocity of the Diaion HPA25 particles. The loaded particles were carried upward by this liquid stream while desorption proceeded. In the liquid–solid separator, the regenerated particles and the effluent were separated. Then, the regenerated particles were returned to the top of the downcomer through the top solids return pipe. During the process of continuous ion exchange, samples were taken from different locations of the columns and BSA concentration was determined by measuring the absorbance at 280 nm using a Cary Bio 50 UV-Visible Spectrophotometer.

Measurement of solids holdup

The solids holdup in the riser and the downcomer was calculated from the pressure gradients in the columns. The pressure gradient in the riser or downcomer column was measured by a manometer as shown in Figure 1 and was given as in Eq. 1

$$\frac{\Delta P}{\Delta z} = \left(1 + \frac{h}{\Delta z}\right)\rho_l g. \tag{1}$$

Given the fact that the liquid velocities in both the riser (U_{lr}) and the downcomer (U_{ld}) are very low (in the range of 10–30 mm/s for U_{lr} and less than 2.0 mm/s for U_{ld}), it is realistic to ignore the pressure drops due to the liquid flow. Therefore, the solids holdup, bed voidage, and pressure gradient can be related as in Eq. 2

$$\frac{\Delta P}{\Delta z} = (\epsilon_s \rho_s + \epsilon_l \rho_l) g. \tag{2}$$

With $\epsilon_s + \epsilon_l = 1$, the relationship between the solids holdup and the pressure gradient is as follows (Eq. 3)

$$\epsilon_s = \frac{(\rho_s - \rho_l)}{\rho_s}\frac{h}{\Delta z}. \tag{3}$$

Maximum adsorption capacity of Diaion HPA25 anion-exchange particles

Maximum adsorption capacity of Diaion HPA25 ion-exchange particles was determined by putting 10 mL swollen Diaion HPA anion-exchange particles into a series of 125-mL flasks containing 25 mL of 10 mM phosphate buffer (pH 7.0) with varying concentrations of BSA. The flasks were then sealed by parafilm "M" (American Can Company) and put on a shaker controlled at 25°C and 200 rpm. After adsorption for 36 h (previous experiments had shown that equilibrium was reached under this condition), the supernatant was centrifuged at 10,000 rpm for 10 min. The protein concentration of the supernatant was analyzed by measuring the absorbance at 280 nm using a Cary Bio-50 UV-Visible Spectrophotometer. The data were interpreted using the Scatchard plot based on a modified Langmuir model (Lan et al., 2000b).

Results and Discussion

Superficial liquid velocity (U_{ld}) and fluidization in the downcomer

The liquid velocity in the downcomer (U_{ld}) is an important parameter for the LSCFB because it can influence the fluidization in the downcomer and the overall throughput of the system. When U_{ld} is maintained in a suitable range, three operating zones are observed in the downcomer which differ in solids holdup, to wit, the dense-phase zone, the dilute-phase zone, and the freeboard zone (Figure 2). The dense-phase zone in the downcomer operates as a conventional fluidized moving bed (Kwauk, 1992) in which solids move down and liquid moves up. The axial solids holdup distribution in such a particulate moving fluidized bed is uniform and the bed expansion can be described by the generalized Richardson and Zaki equation (Richardson and Zaki, 1954; Kwauk, 1992)

$$\frac{U_{ld} + U_{sd}}{U_i} = \epsilon_d^n, \tag{4}$$

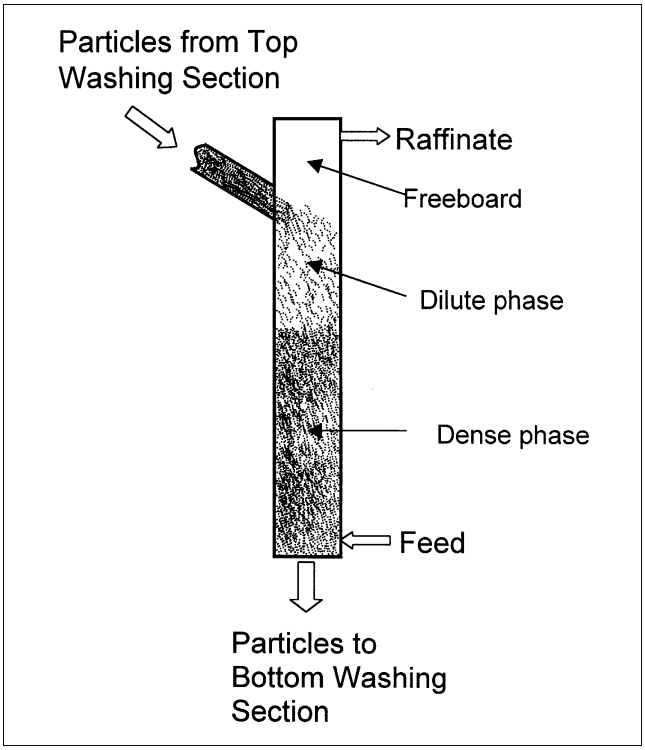

Figure 2. Three zones observed in the downcomer of the LSCFB.

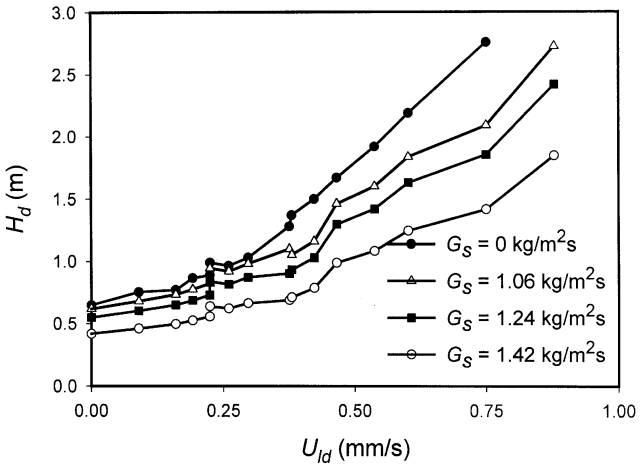

Figure 3. Dependence of downcomer dense-phase height (H_d) on the liquid velocity (U_{ld}) in the downcomer and the solids circulation rate (G_s), with a total of 3.0 kg Diaion HPA25 anion-exchange particles in the LSCFB.

where U_{ld} and U_{sd} are the liquid velocity and the solids velocity in the downcomer, respectively; ϵ_d is the bed voidage in the downcomer; and the bed expansion index, n, can be determined experimentally or from the following correlation

$$n = \left(4.4 + 18\frac{d_p}{D}\right) Re_t^{-0.1}. \quad (5)$$

The dilute-phase zone is created when the ion-exchange particles are fed into the downcomer through the solids entrance when the surface of the dense-phase zone is lower than the solids entrance. The solids holdup in this section is determined by the solids circulation rate. When G_s is zero, the solids holdup in this section is zero. Since the stable operating G_s is small in the LSCFB system, the solids holdup in the dilute-phase zone is lower than that in the dense-phase zone. Similar to other liquid–solid conventional fluidized beds, the solids holdup in the freeboard is nearly zero. There is a clear interface between the freeboard and the dilute-phase zone. Under most conditions, there also exists an interface between the dilute-phase zone and the dense-phase zone. When G_s is very large and solids holdup of the dense phase is low, however, the interface may disappear, because the difference between the solids holdups of these two zones is not so evident.

The extent of the dense phase, the dilute phase, and the freeboard depends on the values of U_{ld} and G_s for a constant amount of particles in the system. As shown in Figure 3, the dense-phase height (H_d) increases with the liquid velocity in the downcomer (U_{ld}) and decreases with the increase of the solids circulation rate (G_s). When the height of the dense-phase zone is increased to the location of the solids entrance on the downcomer, the dilute-phase zone will be overlapped by the dense phase. Under these conditions, the downcomer will have only two zones: the dense phase and the freeboard. The freeboard, however, is an essential component of the downcomer for preventing the loss of ion-exchange particles. The values of U_{ld} and G_s should therefore be maintained in a range that guarantees a certain length of the freeboard.

In terms of protein adsorption in the downcomer, the dense-phase zone is the most important zone, since most of the ion-exchange particles are in this zone and the protein remaining in the liquid phase in the dilute-phase zone and the freeboard should be very low under a nonbreakthrough adsorption condition. Therefore, both the bed height (H_d) and the solids holdup of the dense phase (ϵ_{sd}) are important parameters for the protein adsorption in the downcomer.

When the total amount of the ion-exchange particles circulating in the LSCFB is constant, the dense-phase height in the downcomer at steady state is dependent mainly on three factors: the liquid velocities in the riser (U_{lr}) and downcomer (U_{ld}), and the solids circulation rate (G_s). As discussed earlier, U_{ld} directly affects the bed expansion of the particles in the downcomer and hence the dense-phase height. On the other hand, U_{lr} and G_s influence the number of ion-exchange particles available for the downcomer dense phase when the total number of particles is constant. The higher the U_{lr} and the G_s, the fewer particles are available for the downcomer dense phase, as more particles are circulating in other parts of the LSCFB system.

Superficial liquid velocity (U_{lr}) and the solids holdup in the riser

As discussed before, the riser of the LSCFB system operates in the circulating fluidization regime where particles are carried up by the liquid along the riser and compensated by

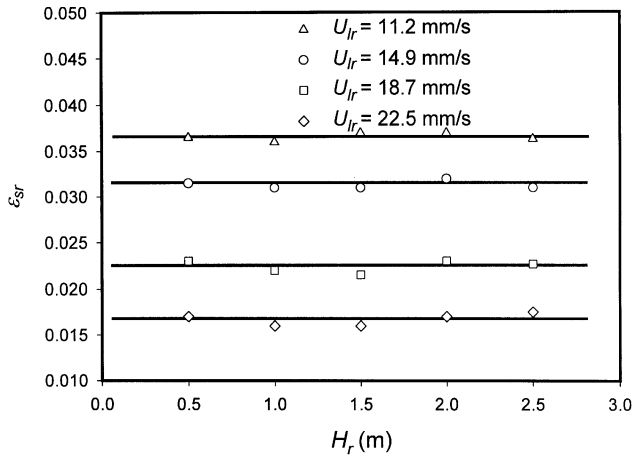

Figure 4. Axial distribution of the solids holdup in the riser.

U_{ld} = 0.6 mm/s.

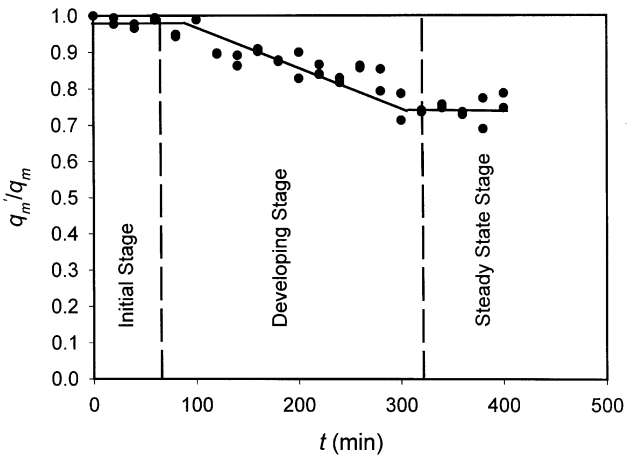

Figure 6. Regeneration of Diaion HPA25 in the riser as a function of operating time.

U_{ld} = 0.6 mm/s, U_{lr} = 11.3 mm/s, G_s = 1.24 kg/m^2·s, H_d = 0.8 m, C_{0d} = 2 g/L.

the continuous feeding of particles into the base through the bottom solids return pipe. Figure 4 shows that the axial solids holdup distribution of Diaion HPA25 is uniform along the riser. This result is in agreement with those previously reported by Liang et al. (1997) and Zheng et al. (1999).

Figure 5 shows the influence of the superficial liquid velocity (U_{lr}) and the solids circulation rate (G_s) on the solids holdup in the riser (ϵ_{sr}). It is clear that at a given U_{ir}, ϵ_{sr} increases with the increase in G_s. On the other hand, for a given G_s, ϵ_{sr} decreases with the increase of U_{lr}. It is worth noting that for a specific G_s, the U_{lr} must be maintained above a critical value. In other words, if U_{lr} is lower than the critical value, the specified G_s is unachievable. This is shown in Figure 5 as the low solids circulation region. The conventional fluidization region shown in Figure 5 is the region where U_{lr} is so low that G_s = 0 (no solids circulation). That is, the riser operated in this region in the conventional fluidization regime.

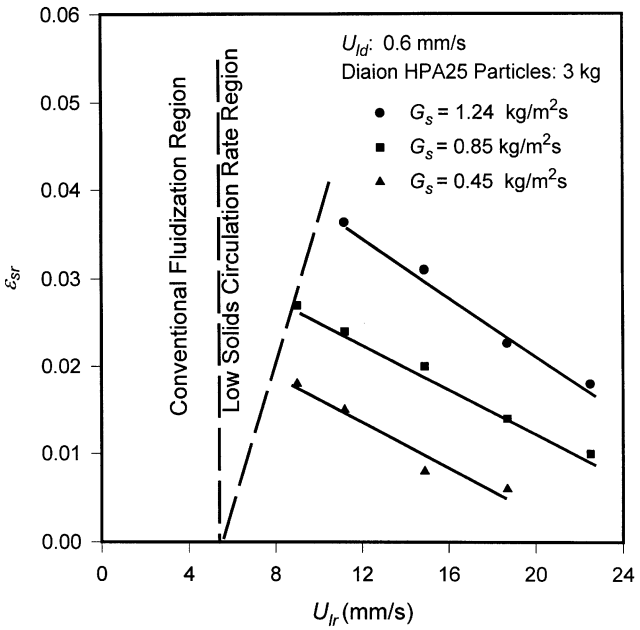

Figure 5. Influences of superficial liquid velocity in the riser (U_{lr}) and solids circulation rate (G_s) on solids holdup in the riser (ϵ_{sr}).

U_{ld} = 0.6 mm/s.

Regeneration of Diaion HPA25 in the LSCFB system

The regeneration of the ion-exchange particles in the LSCFB system was carried out in the riser. The extent of regeneration is a very important parameter for the stable operation of the system. The maximum capacity of regenerated ion-exchange particles as an indication of the extent of the regeneration is one of the key factors influencing the dynamic adsorption capacity of the system. To measure the extent of regeneration, samples of regenerated ion-exchange particles were taken from the liquid–solids separator and the maximum BSA adsorption capacities of those regenerated particle samples (q_m') were measured. Figure 6 shows the change in the maximum capacity of the regenerated ion-exchange particles with time of operation in the LSCFB. In the initial stage, the normalized maximum capacity of the regenerated ion-exchange particles (q_m'/q_m) was approximately 1.0. This was due to the fact that the particles carried up into the separator in the initial stage were only the fresh ion-exchange particles initially packed in the bottom solids return pipe. Those particles did not come in contact with the feed before they were transported to the riser. In the development stage, however, the regeneration rate decreased with time, indicating that a part of the adsorption capacity was lost due to fouling and the incomplete regeneration. However, the normalized maximum capacity was stabilized in the steady-state stage at around 0.75.

It is interesting to find that, after five consecutive runs, with a total treatment volume of about 900 L feed (representing a feed/particle ratio of 300 L/kg), the q_m' of the regenerated ion-exchange particles was still at approximately 62 mg/mL, representing a stabilized q_m'/q_m value of around

0.7. This result indicates that although the BSA adsorption capacity of the fresh Diaion HPA25 anion-exchange particles was decreased by almost 30% in the first run, likely due to fouling and incomplete regeneration, a steady state of regeneration was achieved so that the maximum protein adsorption capacity of the regenerated particles remained stable thereafter. This is an important result for the long-term, stable operation of the system. For practical operations, a portion of the ion-exchange particles could be periodically replaced with fresh particles.

Dynamic adsorption capacity of the system (D)

Protein loading rate is the amount of proteins loaded onto the LSCFB system in a unit time. It can be calculated as follows

$$L = Q_d C_0 = A_d U_{ld} C_0, \tag{6}$$

where Q_d is the flow rate of feed and A_d the cross-sectional area of the downcomer. For a particular LSCFB system, A_d is a constant so that L is proportional to U_{ld} and C_0. Higher protein loading rates will increase the system throughput. However, protein loss through the raffinate will occur when the protein loading rate is higher than the adsorption capacity of the ion exchanger.

The dynamic adsorption capacity of the LSCFB system (D) is defined as the amount of protein adsorbed onto the ion exchangers in the downcomer under the maximum allowable protein loading rate. The maximum allowable protein loading rate is defined here as the maximum protein loading rate for given operating conditions beyond which significant leakage of protein will happen. The dynamic adsorption capacity of an LSCFB system is determined by four major factors: the maximum BSA adsorption capacity of the regenerated ion-exchange particles (q'_m), the solids circulation rate (G_s), the fluidization and backmixing, in the downcomer, and the adsorption equilibrium in the downcomer, particularly in the dense-phase zone. The dynamic adsorption capacity of the downcomer could thus be calculated as follows

$$D = \frac{\kappa G_s A_r q'_m}{\rho_s \epsilon_{mf}} = L_{\max} - (Q_d C_{ed})_{\max} = \left[L Q_d (C_0 - C_{ed}) \right]_{\max}, \tag{7}$$

where A_r is the cross-sectional area of the riser and κ is a lumped correction factor determined by the fluidization, the backmixing, and the adsorption equilibrium in the dense-phase particulate bed in the downcomer. If there is no backmixing (plug flow) for both liquid and solids in the dense-phase zone, and if the mass transfer is very fast so that the adsorption equilibrium is achieved instantly, then κ is one. Otherwise, κ is a constant less than 1. In addition, ρ_s, ϵ_{mf}, and A_r are all constant for a given LSCFB system. Therefore, the dynamic adsorption capacity of an LSCFB system is proportional to G_s and q'_m. The subscript max indicates the conditions of maximum allowable loading rate.

The dynamic adsorption capacity of an LSCFB system represents the upper limit of the protein loading rate of a particular system. In other words, if the actual protein loading rate is larger than the dynamic adsorption capacity of the system, the ion-exchange particulate bed in the downcomer will be "broken through" and a significant amount of proteins will leak into the raffinate.

A unique feature of the LSCFB system is that it is suitable for the adsorption using ion-exchange particles with relatively low adsorption capacity. Because loaded ion-exchange particles are continuously regenerated in this system, the low capacity of ion-exchange particles can be compensated for to a certain extent. As discussed earlier, the dynamic adsorption capacity of the system is determined by the q'_m, G_s, and the fluidization in the dense phase. Therefore, with good fluidization and a relatively large G_s, a reasonably large magnitude of dynamic adsorption capacity of the LSCFB system can be achieved, even for ion-exchange particles with a relatively low adsorption capacity.

Influence of operating conditions on BSA adsorption ratio in the downcomer

The protein adsorption ratio in the downcomer, X_d, is determined by the following equation

$$X_d = \frac{(C_{0d} - C_{ed})}{C_{0d}}, \tag{8}$$

where C_{0d} and C_{ed} are the protein concentrations in the feed and the raffinate, respectively.

A very important parameter that influences the protein adsorption in the downcomer is G_s. The experimental results of BSA adsorption in the downcomer under conditions of C_{0d} = 2 g/L, U_{ld} = 0.6 mm/s, U_{lr} = 11.3 mm/s, and various G_s are shown in Figure 7. It was clear that G_s had significant effects on the BSA adsorption. At a high G_s of 1.42 kg/m^2·s, almost all BSA in the feed (98%) was removed. When G_s was reduced to 1.06 kg/m^2·s, however, only about 70% of the BSA was removed, indicating significant loss of protein.

The remarkable influence of G_s on the protein adsorption in the downcomer can be illustrated by its effects on the dynamic adsorption capacity of the system. As discussed earlier,

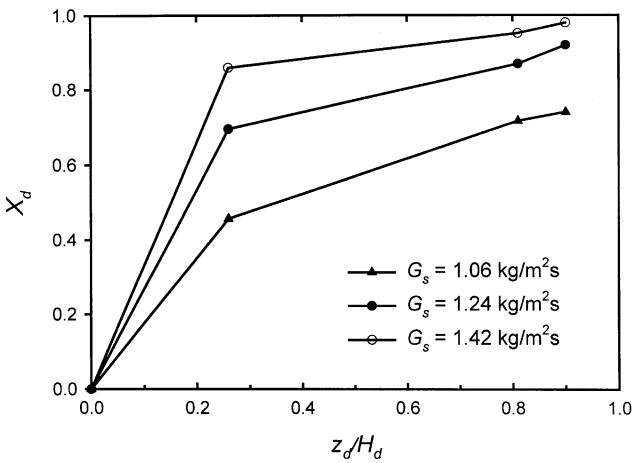

Figure 7. Effects of solids circulation rate on characteristics of BSA adsorption in the downcomer.

U_{ld} = 0.6 mm/s, U_{lr} = 11.3 mm/s, H_d = 0.8 m, C_{0d} = 2 g/L.

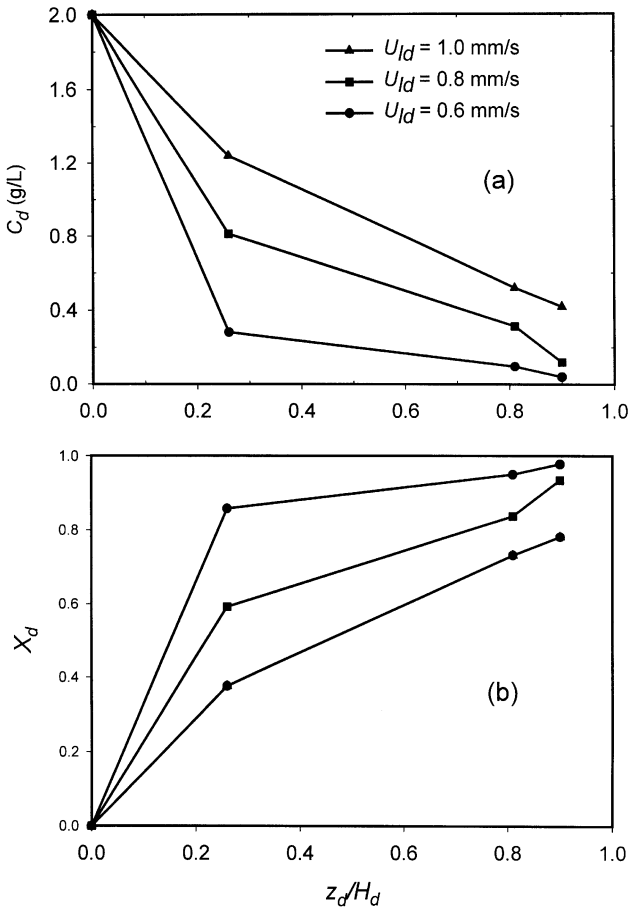

Figure 8. Effects of superficial liquid velocity (U_{ld}) on the characteristics of BSA adsorption onto Diaion HPA25 anion exchange particles in the downcomer.

U_{lr} = 11.3 m/s, G_s = 1.24 kg/m^2·s, H_d = 0.8 m, C_{0d} = 2 g/L: (a) BSA concentration profiles; (b) BSA adsorption ratio profiles.

the dynamic adsorption capacity of an LSCFB system is proportional to G_s. The system thus has a higher dynamic capacity at G_s = 1.42 kg/m^{2}s than that at G_s = 1.06 kg/m^{2}s. In other words, the results indicate that the actual protein loading rate at the tested condition (U_{ld} = 0.6 mm/s and C_0 = 2 g/L) was higher than the dynamic adsorption capacity (the maximum allowable protein loading rate) of the system at the conditions of G_s = 1.06 kg/m^{2}s and U_{ld} = 0.6 mm/s so that a significant protein loss occurred under those conditions.

The influence of the liquid velocity in the downcomer (U_{ld}) on the BSA adsorption is shown in Figures 8a and 8b. The experiments were carried out under conditions of C_{0d} = 2 g/L, U_{lr} = 11.3 mm/s, G_s = 1.42 kg/m^{2}s, and various U_{ld}. The height of the dense phase in the downcomer was carefully maintained at 0.8 m by controlling the number of Diaion HPA25 particles in the system. When U_{ld} increased from 0.6 mm/s to 1.0 mm/s, the protein concentration in the raffinate increased from 0.04 g/L to 0.42 g/L (Figure 8a) and the adsorption ratio in the downcomer decreased accordingly from 98% to 79% (Figure 8b), indicating that a significant protein leakage happened at conditions U_{ld} = 10 mm/s. The influence of U_{ld} on the protein adsorption in the downcomer was as follows: (1) It directly influences the protein loading rate. The protein loading rate increases proportionally with the increase of U_{ld}. (2) It affects the fluidization and backmixing of ion-exchange particles in the dense phase, which in turn influence the dynamic adsorption capacity of the system. The influence of U_{ld} on the dynamic adsorption capacity is a somewhat complicated issue. While the increase in U_{ld} increases the bed height of the dense phase, which is beneficial for a higher dynamic adsorption capacity, it also increases backmixing, which tends to reduce the dynamic adsorption capacity.

Effects of operating conditions on BSA desorption ratio in riser and overall BSA recovery

The protein desorption ratio in the riser is defined by the following equation

$$X_r = \frac{(q_{0r} - q_{er})}{q_{0r}}, \tag{9}$$

where q_{0r} and q_{er} are protein concentrations in the solid phase at the solids entrance of the riser and in the separator, respectively. However, q_{0r} and q_{er} are usually difficult to measure. It is much more convenient to obtain the protein desorption ratio in the riser by the following equation

$$X_r = \frac{X}{X_d}, \tag{10}$$

where X is the overall protein recovery of the LSCFB system and X_d is the protein adsorption ratio in the downcomer. The overall protein recovery is the ratio between the protein output flux in the extract and the input flux (the loading rate) in the feed. It can be calculated by the following equation

$$X = \frac{Q_r C_{er}}{Q_d C_{0d}}, \tag{11}$$

where Q_r and Q_d are the liquid flow rates in the riser and the downcomer, respectively, C_{er} is the protein concentration in the extract, and C_{0d} is the protein concentration in the feed.

The effects of U_{lr} on the adsorption in the riser were investigated under C_{0d} = 2 g/L, U_{ld} = 0.6 mm/s, G_s = 1.24 kg/m^{2}s, and various U_{lr}. The results are shown in Figure 9a and 9b. When other conditions, such as the solids circulation rate and protein concentration in the entering particles, were constant, the protein concentration in the extract decreased significantly with the increase in the superficial liquid velocity in the riser (Figure 9a). This is because at higher U_{lr}, the same amount of protein recovered was diluted by more extract buffer. As shown in Figure 9b, however, the increase of U_{lr} resulted in an increase in the overall recovery rate.

Stable operation window: Hydrodynamic aspects

For a continuous system, one of the keys is how to achieve and maintain a stable and steady-state operation. There are two aspects of the stable operation of the LSCFB system: hydrodynamic stability and kinetic stability. The achievement

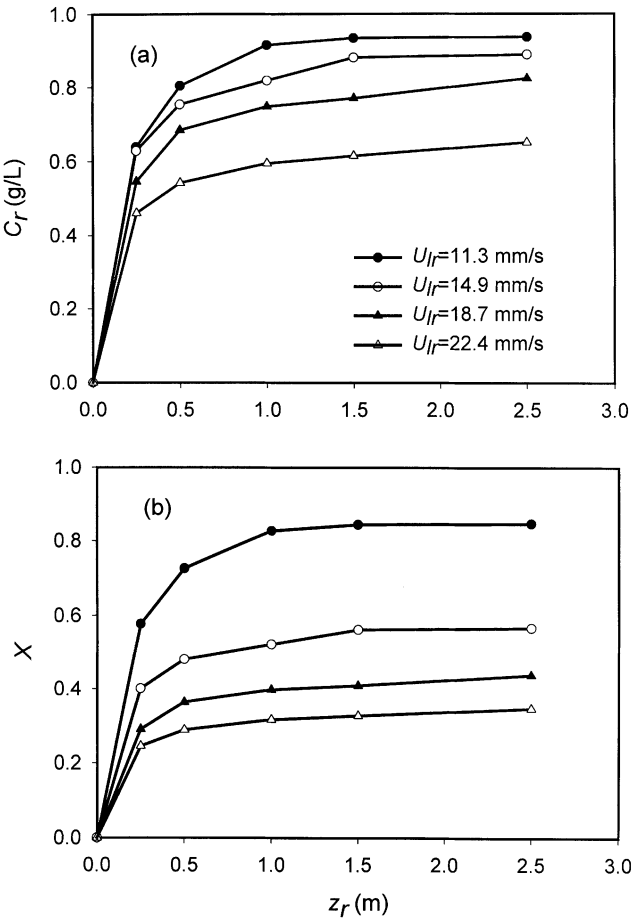

Figure 9. The effects of superficial liquid velocity (U_{lr}) on the characteristics of BSA desorption from Diaion HPA25 anion exchange particles in the riser.

U_{ld} = 0.6 m/s, G_s = 1.24 kg/m^2·s, H_d = 0.8 m, C_{0d} = 2 g/L: (a) BSA concentration profiles; (b) BSA desorption ratio profiles.

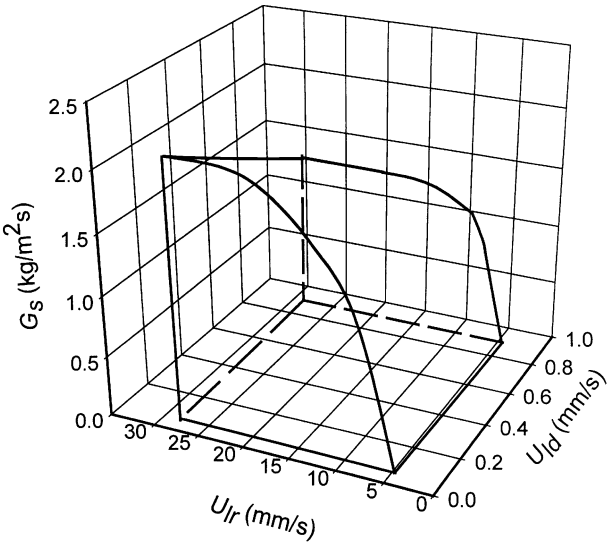

Figure 10. Hydrodynamic stable operation window of the LSCFB system with 3-kg Diaion HPA25 ion-exchange particles.

The fluidization liquid in the riser was 0.4 M NaCl buffer and in the downcomer tap water.

and maintenance of hydrodynamic steady state are the prerequisite of the kinetic steady state. The hydrodynamic stable operating window for our particular system with respect to operating conditions U_{ld}, U_{lr}, and G_s is shown in Figure 10. Although the hydrodynamic stable operating window is very system-dependent, some generalized principles exist and are as follows.

Superficial Liquid Velocity in the Downcomer (U_{ld}). The superficial liquid velocity in the downcomer (U_{ld}) is one of the most important operation conditions affecting the stability of the system. The influence of U_{ld} includes the following two aspects: (1) the fluidization in the dense-phase section; and (2) the passage of particulates in the feed through the ion-exchange bed. Therefore, the liquid velocity in the downcomer should be large enough to fluidize the ion-exchange bed to provide enough voidage for the passage of the particulates in the feed. If U_{ld} is lower than the limit just cited, particulates in the broth will be retained in the bed and the whole column will eventually become plugged.

On the other hand, the liquid velocity in the downcomer should not be larger than the terminal velocity of the ion-exchanger particles to allow the particles to fall down in the downcomer. Furthermore, to prevent the loss of ion-exchange particles, U_{ld} should be in such a magnitude that a section of freeboard is maintained in the downcomer. In this particular LSCFB system, the maximum U_{ld} was determined to be 0.9 mm/s, representing a maximum flow rate (feed plus bottom wash water) of 36.5 L/h.

Superficial Liquid Velocity in the Riser (U_{lr}). Superficial liquid velocity in the riser (U_{lr}) is another important operation condition with significant influence on the stability of the system. The U_{lr} must be higher than the terminal velocity of ion-exchange beads in order to operate the riser in the circulating fluidization regime. The terminal velocity of Diaion HPA25 beads was determined to be 4.5 mm/s.

Too large a U_{lr}, however, will destabilize the system because too many ion-exchange particles will accumulate in the liquid–solid separator. When the liquid velocity in the riser is close or higher than the terminal velocity of the particles, the particles cannot be transferred into the downcomer. The maximum U_{lr} for this system was determined to be 29.3 mm/s.

Solids Circulating Rate (G_s). The solids circulating rate (G_s) is, as discussed previously, an important parameter contributing to the dynamic adsorption capacity of the system: the higher the G_s, the larger the dynamic adsorption capacity of the system. The G_s is also a very important parameter for the maintenance of the dynamic seal between the riser and the downcomer. As discussed previously, the dynamic seal between the riser and the downcomer is maintained by keeping the solids return pipes in the packed moving-bed regime. At steady state, the number of particles transferred into the solids return pipe from the downcomer, which is determined by the downward solids flux in the downcomer, equals the particles transferred to the riser, which is determined by the

upward solids flux in the riser. If, under the given conditions, the upward solids flux represented by G_s in the riser is larger than the maximum possible downward solids flux in the downcomer, the solids holdup in the bottom solids return pipe will be reduced to make up the balance. If this condition continues, the solids holdup in the solids return pipe will eventually become so low that the dynamic seal cannot be maintained.

Removal of contaminants from product streams

Results from this study as described earlier have shown that the LSCFB system is an excellent technique for continuous protein recovery. In addition, because of the unique features associated with the LSCFB (high adsorption efficiency, applicability to unclarified streams, and so on), the system is also suitable for the removal of contaminant ions from substrate, product, or intermediate product streams. For instance, with the use of appropriate ion-exchange particles, the LSCFB system will be very efficient for the deionization of water and for the removal of contaminants from fructose syrups.

Conclusions

In this research, an LSCFB system has been developed and successfully demonstrated for us in continuous BSA protein extraction. Hydrodynamic studies showed that the LSCFB system was stable and suitable for the continuous protein recovery. It was found that the downcomer could be divided into three zones according to the solids holdup: the dense-phase zone, the dilute-phase zone, and the freeboard. The dense phase is the most important zone for protein adsorption and the freeboard is an essential component for preventing the loss of ion-exchange particles. Continuous BSA adsorption and desorption and regeneration of ion-exchange particles in the system were studied with respect to the influence of different operating conditions. Typical operating parameters for the LSCFB are summarized in Table 2. Under these conditions, results regarding the continuous BSA recovery using this system indicated a high protein removal efficiency of up to 98% and a overall protein recovery of up to 84%. The LSCFB system is thus promising for both protein recovery and the removal of contaminants from products or intermediate products.

Table 2. Parameters for the Continuous BSA Recovery in the LSCFB System under Typical Operating Conditions

Flow rate of the extracting buffer (Q_r, L/min)	0.3
Flow rate of the feed (Q_d, L/min)	0.64
Superficial liquid velocity in the riser (U_{lr}, mm/s)	11.3
Superficial liquid velocity in the downcomer (U_{ld}, mm/s)	0.6
Solids circulation rate (G_s, kg/m^{2}s)	1.42
BSA concentration in the feed (C_0, g/L)	2
Height of the riser column (H_r, m)	3
Height of the dense phase in the downcomer (H_d, m)	0.8
Solids holdup in the riser (ϵ_r)	0.035
Solids holdup in the downcomer (ϵ_d)	0.34
Diaion HPA25 regeneration ratio (R, %)	0.734
BSA desorption ratio in the riser (X_r)	0.86
BSA adsorption ratio in the downcomer (X_d)	0.98
Overall BSA recovery (X)	0.84
BSA concentration at the extract outlet (C_{er}, g/L)	0.79
BSA concentration at the raffinate outlet (C_{ed}, g/L)	0.04

Note: Results shown are the average of three parallel experiments.

Acknowledgment

Financial support from the Natural Science and Engineering Research Council of Canada (NSERC) through a Strategic Grant to A.M., A.B., and J.Z. is gratefully acknowledged. In addition, Q. Lan was supported by an OGGST scholarship.

Notation

A = cross-sectional area of a column, m^2
C = concentration of BSA in the liquid phase, g/L or kg/m^3
d_p = particle mean diameter, m
D = dynamic adsorption capacity of the LSCFB system, g BSA/s or g BSA/h
G_s = solids circulation rate, kg/m^{2}s
H_r = riser height, m
H_d = dense-phase height in the downcomer, m
L = protein loading rate, g/s or kg/s
Q = flow rate of liquid in a column, m^3/s or L/min
q = concentration of protein in solids phase, g/L or kg/m^3
q_m = maximum BSA adsorption capacity of the ion-exchange particles, g/L or kg/m^3
q'_m = maximum BSA adsorption capacity of the regenerated ion-exchange particles, g/L or kg/m^3
R = regeneration rate of ion-exchange particles, dimensionless
t = time, s
U_l = superficial liquid velocity, mm/s
U_m = minimal fluidization velocity, mm/s
U_s = superficial solids velocity, mm/s
U_t = particle terminal velocity, mm/s
X = overall protein recovery
X_d = protein adsorption ratio in the downcomer
X_r = protein desorption ratio in the riser
z = distance from the bottom of a column, m

Greek letters

ϵ_l = bed voidage, dimensionless
ϵ_s = solids holdup, dimensionless
ρ = density, kg/m^3
κ = equation constant, dimensionless

Subscripts

d = downcomer
e = exit
l = liquid phase
r = riser
s = solids phase
max = conditions under maximum loading rate
0 = inlet (initial)

Literature Cited

Burns, M. A., and D. J. Graves, "Continuous Affinity Chromatography Using a Magnetically Stabilized Fluidized Bed," *Biotechnol. Prog.*, **1**, 95 (1995).

Byers, C. H., W. G. Sisson, T. S. Snyder, R. J. Beleski, U. P. Nayak and T.L. Francis," Zirconium and Hafnium Separation in Sulfate Solutions Using Continuous Ion Exchange Chromatography," U.S. Patent No. 5,618,502 (1997).

Chase, H. A., "Purification of Proteins by Adsorption Chromatography in Expanded Beds," *TIBTECH*, **12**, 296 (1994).

Draeger, N. M., and H. A. Chase, "Liquid Fluidized Bed Adsorption of Protein in the Presence of Cells," *Bioseparation*, **2**, 67 (1991).

Gordon, N. F., H. Tsujimura, and C. L. Cooney, "Optimization and Simulation of Continuous Affinity Recycle Extraction," *Bioseparation*, **1**, 9 (1990).

Higgins, I. R., "Continuous Ion Exchange of Process Water," *Chem. Eng. Prog.*, **65**, 59 (1969).

Himsley, A., "Continuous Countercurrent Ion Exchange Process," U.S. Patent No. 4,279,755 (1981).
Kwauk, M., *Fluidization: Idealized and Bubbleless, with Applications*, Science Press, Beijing and New York; Ellis Horwood, Toronto (1992).
Lan, Q., J.-X. Zhu, A. S. Bassi, A. Margaritis, Y. Zheng, and G. E. Rowe, "Continuous Protein Recovery Using a Liquid-Solid Circulating Fluidized Bed Ion Exchange System: Modelling and Experimental Studies," *Can. J. Chem. Eng.*, **78**, 82 (2000).
Lan, Q., A. S. Bassi, J.-X. Zhu, and A. Margaritis, "A Modified Langmuir Model for the Prediction of the Effects of Ionic Strength on the Equilibrium Characteristics of Protein Adsorption onto Ion Exchange/Affinity Adsorbents," *Chem. Eng. J.*, **81**, 179 (2001).
Liang, W.-G., S. L. Zhang, J.-X. Zhu, J. Yong, Z. Q. Yu, and Z. W. Wand, "Flow Characteristics of the Liquid-Solid Circulating Fluidized Bed," *Powder Technol.*, **90**, 95 (1997).
Porter, R. R., "Continuous Ion Exchange Process and Apparatus," U.S. Patent No. 3,879,287 (1975).
Pungor, E., N. B. Afeyan, N. F. Gordon, and C. L. Cooney, "Continuous Affinity-Recycle Extraction: A Novel Protein Separation Technique," *Bio/Technol.*, **5**, 604 (1987).
Richardson, J. F. and W. N. Zaki, "Sedimentation and Fluidization," *Trans. Inst. Chem. Eng.*, **32**, 35 (1954).
Rodrigues, M. I., C. A. Zaror, F. Maugeri, and J. A. Asenjo, "Dynamic Modelling, Simulation and Control of Continuous Adsorption Recycle Extraction," *Chem. Eng. Sci.*, **47**, 263 (1992).
Rowe, G. E., A. Margaritis, Q. Lan, A. S. Bassi, and J.-X. Zhu, "A New Kinetic Model of Protein Adsorption on Suspended Anion-Exchange Resin Particles," *Biotechnol. Bioeng.*, **65**(6) 613 (1999).
Slater, M. J. and P. Prud'homme, "Continuous Ion Exchange in Fluidized Beds." *Can. Mines Bur.*, *Tech. Bull.*, **158**, 1 (1972).
Turner, J. C. R. and M. R. Church, "A Continuous Ion Exchange Column," *Trans. Inst. Chem. Eng.*, **41**, 283 (1963).
Zheng, Y., J.-X. Zhu, J. Wen, S. Martin, A. S. Bassi, and A. Margaritis, "Hydrodynamic Behavior in a Liquid-Solid Circulating Fluidized Bed," *Can. J. Chem. Eng.*, **77**, 284 (1999).
Zheng, Y. and J.-X. Zhu, "Overall Pressure Balance and System Stability in a Liquid-Solid Circulating Fluidized Bed," *Chem. Eng. J.*, **79**(2), 145 (2000).
Zhu, J.-X., Y. Zheng, D. G. Karamanev, and A. S. Bassi, "(Gas)-Liquid-Solid Circulating Fluidized Beds and their Potential Applications to Bioreactor Engineering," *Can. J. Chem. Eng.*, **78**, 82 (2000).

Manuscript received May 16, 2000, and revision received Dec. 11, 2000.